Braess's Paradox Analog in Physical Networks of Optimal Exploration

Georgios Gounaris[1] and Eleni Katifori[1,2]
[1]Department of Physics and Astronomy, University of Pennsylvania, Philadelphia, Pennsylvania 19104, USA
[2]Center for Computational Biology, Flatiron Institute, New York, New York 10010, USA

(Received 30 April 2023; revised 31 January 2024; accepted 2 July 2024; published 9 August 2024)

In stochastic exploration of geometrically embedded graphs, intuition suggests that providing a shortcut between a pair of nodes reduces the mean first passage time of the entire graph. Counterintuitively, we find a Braess's paradox analog. For regular diffusion, shortcuts can worsen the overall search efficiency of the network, although they bridge topologically distant nodes. We propose an optimization scheme under which each edge adapts its conductivity to minimize the graph's search time. The optimization reveals a relationship between the structure and diffusion exponent and a crossover from dense to sparse graphs as the exponent increases.

DOI: 10.1103/PhysRevLett.133.067401

Time is a limiting factor for a plethora of physical networks that rely on diffusion as a mechanism of transport and search. Diffusive exploration can describe Euclidean space trajectories in various length scales, e.g., foraging animals searching for food or molecules searching for a binding target [1]. Diffusion is also used to describe stochastic transitions between the numerous metastable states in an energy landscape [2,3]. In all of these different systems, the average timescale in which a random walker will encounter a target for the first time is given by the mean first passage time (MFPT) [4].

The diffusive exploration of complex networks is inherently linked to the structural properties of the graph [5,6]. For instance, a random walk on a regular lattice becomes transient in dimensions higher than 2. This is only a preamble to the rich phenomenology of diffusion in real-world networks that exhibit hierarchical structures that strongly differentiate the graph's effective dimension from that of the embedding space [7]. Small-world structures present in social and neuronal networks [8], or self-similar structures such as intracellular networks [9], are some examples of complex architectures.

In addition to the topological features, the physical properties of a graph, such as the Euclidean edge lengths, can influence the diffusion dynamics. Deviations from uniform edge lengths can induce heterogeneity in transit times between neighboring nodes. Furthermore, waiting times before performing a step may arise due to barriers that hinder the diffusive passage, leading to subdiffusive motion. Conversely, mechanisms of active motion, such as motors, can accelerate the propagation speed, resulting in superdiffusion.

Search efficiency is often crucial for the survival of the random walker and the functionality of the network, especially in biological systems. This has motivated extensive research on how a node's location and connectivity can affect the node's search time, which is defined as the MFPT to the target node averaged over all starting nodes also known as the global mean first passage time (GMFPT) [10]. More recently, for planar organelle networks, Ref. [11] studied the effect of loops on the overall network transport, quantified by the GMFPT averaged over all the targets (TA-GMFPT) or intuitively *graph search time*. However, the graph structure that optimizes diffusive search remains unknown.

To improve search efficiency, intuition suggests adding a direct shortcut between topologically distant nodes. This could reduce the MFPT of the pair and create additional pathways for the rest, see Fig. 1(a). Counterintuitively, we find that adding a shortcut can negatively affect the graph search time. This phenomenon is reminiscent of the Braess paradox discovered in the context of road networks in 1968, where creating a shortcut road increases the overall commute time due to congestion [12] (see Supplemental Material [13]). In the context of diffusive search, delays arise not from congestion but rather from the substantial

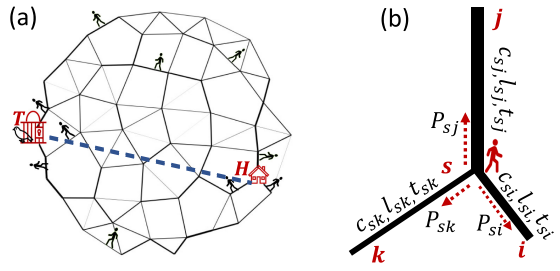

FIG. 1. (a) Sketch of a diffusive search for the absorbing target T, starting at node H. A shortcut (dotted path) affects both the MFPT to the target and the graph search time. (b) A junction on a weighted and spatially embedded graph. The conductivity c_{si} and length l_{si} of each link control the transition probability P_{si} between neighboring nodes.

Euclidean lengths of the shortcuts, which can nonlinearly increase the graph search time. To avoid Braessian-like links, we propose a general optimization scheme in which each edge adjusts its weight to minimize the graph's search time.

In particular, we consider random walks on spatially embedded, weighted graphs of N nodes and N_e edges. Each pair of nodes i,j may be connected by a single edge with weight $w_{ij} = (c_{ij}/l_{ij})$, where $w_{ij} = 0$ implies no connection. Note that the inverse weight can be thought of as the resistance $r_{ij} = w_{ij}^{-1}$ of the edge, in a resistor analog of the random walk [19]. Unlike previous work, see, e.g., [20], here we consider both a length independent c_{ij} (which can be thought of as the conductivity of the edge) and the Euclidean distance between the two nodes l_{ij}. The motion of the particle can be treated as a Markov state model, with each Markov state corresponding to a node neighborhood. Transitions between neighborhoods are memoryless. The probability to directly transit from node i to an adjacent node j is $P_{ij} = (w_{ij}/\sum_j^N w_{ij})$.

In each link, the dynamics are treated as 1D anomalous diffusion, and the mean transit time through a link is $(l_{ij}^{2\beta}/\mathcal{D}_\beta)$, where $\mathcal{D}_\beta$ is the diffusivity. This is the time at which the standard deviation of the random walk displacement equals the edge length $\sqrt{\langle \Delta x^2 \rangle} = l_{ij}$. The anomalous diffusion exponent β captures two distinct regimes: $\beta < 1$ for superdiffusive motion and $\beta > 1$ for subdiffusion [21]. The (weighted) waiting time to transit from i to any neighboring node is $\tau_i \equiv \sum_j^N w_{ij}(l_{ij}^{2\beta}/\mathcal{D}_\beta)$.

We consider the trapping problem of continuous time random walks in a weighted graph G when a target node y is a perfect absorber. The MFPT from node i to the target can be expressed using the truncated weighted Laplacian $\boldsymbol{\mathcal{L}}$ as $T_{i\to y} = \sum_{j,j\neq y}^{N-1} \mathcal{L}_{ij}^{-1}\tau_j$ [22,23]. From the graph Laplacian defined as $L_{ij} = -w_{ij}$ for $i \neq j$ and $L_{ii} = \sum_j^N w_{ij}$, we obtain the truncated $\boldsymbol{\mathcal{L}}$ after deleting the yth row and column that contain the zero escape weights of the absorbing node, notably $\boldsymbol{\mathcal{L}}$ is invertible. We also remove the yth row of $\boldsymbol{\tau}$ that corresponds to the waiting time of the trap. Equivalently, the MFPT can be derived by replacing the edge weights w_{ij} with the transition probabilities P_{ij}, leading to a normalized Laplacian and a mean waiting time (see Supplemental Material [13]).

To estimate the efficiency of diffusive search on graph G we study the graph search time as the average MFPT over all pairs of initial and target nodes $\langle T \rangle = [1/N(N-1)]\sum_y^N \sum_{i,i\neq y}^{N-1} T_{i\to y}$. Spectral analysis simplifies this double sum, expressing $\boldsymbol{\mathcal{L}}^{-1}$ as a function of the nonzero eigenvalues $\lambda_k > 0$ for $k > 1$ and the corresponding eigenvectors of the Laplacian $\boldsymbol{L}$ [20]. These eigenvalues are related to the effective resistance of the graph [24], as follows:

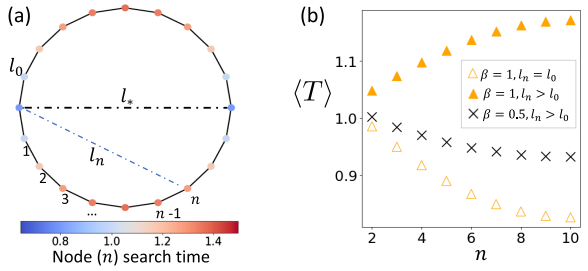

FIG. 2. (a) Diffusive search in a 1D circular lattice of $N = 20$ nodes labeled by their topological distance n from node 0. Without shortcuts, all the nodes on the circle have equal search times. The heat map shows each node's search time defined as $[1/(N-1)]\sum_{i,i\neq n}^{N-1} T_{i\to n}$, after adding the longest chord l_*. (b) The graph search time $\langle T \rangle$ after adding a shortcut of length l_n is normalized by the ring's search time without the shortcut and is plotted as a function of topological distance n. For diffusion $\beta = 1$, if all the edges are assigned equal lengths ($l_n = l_0$), a shortcut always improves the graph search time (empty triangles). However, when the edge lengths are determined by the node Euclidean distances ($l_n > l_0$), any shortcut on the circle increases the graph search time (filled triangles). The Braess's paradox resolves for ballistic propagation ($\beta = 0.5$) as the shortcuts improve the search despite their long lengths (crosses).

$$R = N\sum_{k=2}^{N}\frac{1}{\lambda_k}. \tag{1}$$

Here $R = \sum_{i>j} R_{ij}$ and R_{ij} is the effective resistance between nodes i, j if a unit current is inserted on i and retrieved at j and the voltage drop represents the MFPT [19]. Finally, we can derive a relation for the graph search time that reveals the interplay between diffusion and the graph structure:

$$\langle T \rangle = \frac{R}{N(N-1)}\sum_{i,j}^{N} w_{ij}\frac{l_{ij}^{2\beta}}{\mathcal{D}_\beta}, \tag{2}$$

the sum is the overall edge transit time and depends on the anomalous diffusion exponent β (see Supplemental Material [13]).

To examine the impact of topological modifications on the diffusive search efficiency of the graph, we consider circular graphs with lattice constant l_0, see Fig. 2(a). Two non-neighboring nodes separated by $n > 1$ edges in the original lattice can be directly linked with a shortcut s_n. We distinguish two cases: nonspatially embedded graphs where all the edges are assigned equal lengths $l_n = l_0$ and spatially embedded networks where the edge lengths can be heterogeneous depending on the Euclidean distance between nodes.

If all the edge lengths are equal then the transit time through each link is the same: $(l_0^{2\beta}/\mathcal{D}_\beta)$. This is analogous to a superdiffusive $\beta = 0$, for which the edge transit time does not depend on the length. For equal lengths and fixed

sum of weights $\sum_{i,j}^{N} w_{ij} = 1$, the graph search time becomes $\langle T \rangle = [l_0^{2\beta}/N(N-1)\mathcal{D}_\beta]R$, which is a convex function of the weights (or c_{ij}, as $l_{ij} = \text{const}$) [24]. In this case, the optimal search architecture is a fully connected graph with uniform edge weights [25].

However, in most physical networks there is heterogeneity in the length and conductivity distributions. A periodic 1D lattice embedded in the circle can reveal the competing relationship between topology, geometry, and diffusion. Suppose a shortcut s_* with conductivity c_* and length l_* is added between antipodal nodes. This addition will have a twofold effect. While it bridges the most distant nodes, the shortcut's long Euclidean length requires a long transit time.

Counterintuitively, we find that for regular and subdiffusive exploration ($\beta \geq 1$), adding any chord between topologically distant nodes in a circular node embedding increases the total search time, see Fig. 2(b). This is analogous to Braess's paradox, where increasing the available pathways can reduce overall efficiency. Such behavior can occur in physical networks: in traffic networks adding a road can increase the total transportation time [26], or in power grids, adding extra transmission lines could promote blackouts [27].

To find the architecture that minimizes the graph search time $\langle T \rangle$, and eliminates Brassian edges we develop a gradient descent algorithm inspired by the adaptation mechanisms of flow networks [28,29]. During minimization, each edge adapts its conductivity c_{ij} while its length l_{ij} is kept fixed (see Supplemental Material [13]). The updated conductivities at the $n+1$ iteration are $c_{ij}^{n+1} = c_{ij}^n + \delta c_{ij}^n$ and the weights $w_{ij}^{n+1} = (c_{ij}^{n+1}/l_{ij})$. The variation of the conductivities is $\delta c_{ij}^n \approx -v(\partial E/\partial c_{ij}^n)$, where v is the step size and E is the objective function,

$$E = \langle T \rangle + \lambda \left(\sum_{i,j}^{N} w_{ij} - W_{\text{tot}} \right). \tag{3}$$

The Lagrange multiplier λ conserves the sum of the weights W_{tot} during minimization [29].

We allow all possible link connections between pairs of nodes embedded in a circle to ensure full degrees of freedom for approximating the optimal architecture. The initial conductivity of each link is assigned equal to its length $c_{ij}^0 = l_{ij}$ to impose uniform initial weights $w_{ij}^0 = 1$. We then apply the adaptation rule to find the optimal graphs for different values of the diffusion exponent β. To analyze the weighted network features, we employ robust topological measures, including the clustering coefficient C_l [30] and mean shortest path length L [31].

In one dimension, for superdiffusive motion ($\beta < 1$), the optimal network has shortcuts and is highly clustered, see Figs. 3(a) and 3(b). For subdiffusive motion ($\beta \geq 1$), long

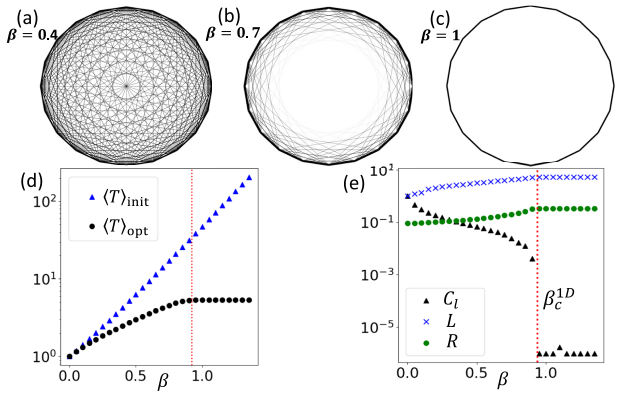

FIG. 3. (a)–(c) Optimal search weights (edge thickness) for different diffusive exponents β, for a complete graph of $N = 20$ nodes regularly placed ($l_0 = 1$) on a circle. As β increases, the long edge weights decrease while the short edge weights increase. For subdiffusion $\beta \geq 1$, only the shortest edges remain. (d) Shows the initial $\langle T \rangle_{\text{init}}$ and optimal $\langle T \rangle_{\text{opt}}$ search times. (e) The weighted mean shortest path length L and the graph effective resistance R increase with β. The weighted clustering coefficient C_l decreases with β, and drops at a minimum for $\beta_c \approx 0.95$ (dashed line). In one dimension, the transition from a dense graph with long-range links to a sparse short-range lattice occurs at $\beta_c = 1$ as $(N \to \infty)$. The crossover exponent β_c is obtained numerically when the clustering plateaus, see Supplemental Material [13].

links vanish and the optimal graph is a 1D ring lattice, with minimal clustering and a large shortest path length. The transition from dense to sparse graphs depends on the system size and occurs asymptotically for $\beta_c = 1$ in one dimension, as $N \to \infty$, see Fig. 4(b). Notably, the crossover occurs at the same β_c for any convex constraint function of the conductivities $\sum_{ij} c_{ij}^\gamma$, $\gamma \geq 1$, and even when the constraint is softened to an upper bound. This indicates that the maintenance or not of an edge is dictated by the graph's search time $\langle T \rangle$ and not by the resource constraint.

The optimization algorithm finds the edge weight distribution that minimizes $\langle T \rangle$, irrespective of the initial edge weight assignment (see Supplemental Material [13]). We further probe the stability using global minimization techniques like basin hopping [32,33], and the obtained minima match those from gradient descent. Our analysis also extends to sparse graphs embedded on regular lattices when the density of added shortcuts is low $[N_e/N(N-1)] \ll 1$. In sparse topologies, the optimal architecture is restricted by the allowed edge connections leading to less efficient minima than those of dense graphs. However, we observe a crossover for subdiffusion ($\beta \geq 1$) regardless of the shortcut density. In a circular embedding, the optimal architecture is the 1D circular graph with minimal edge lengths (see Supplemental Material [13]).

We now test how the optimal search architecture depends on the dimension of the embedding space and the node positions. We study 2D and 3D using square and cubic

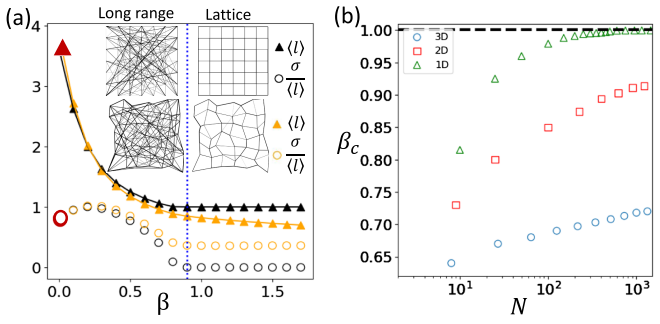

FIG. 4. (a) Shows the mean edge length $\langle l\rangle$ and the coefficient of variation $(\sigma/\langle l\rangle)$, for optimal search networks of $N = 144$ in a regular (black) and a random node embedding (orange). Before optimization, all the edges have uniform weights and the initial $\langle l\rangle$, $(\sigma/\langle l\rangle)$ are shown in red. For β smaller than $\beta_c^{2D} = 0.87$ (dashed line), the optimal graphs (left of the inset, smaller example) have long-range links. For $\beta > \beta_c^{2D}$, there is a crossover at which only the shortest edges survive and the variance of the lengths plateaus at a minimum. Notably, networks with randomized node positions achieve lower average edge lengths than their regular lattice counterparts. (b) The crossover occurs at different exponents β_c depending on the system size N, and the dimension of the lattice embedding. Here, each β_c is numerically determined when $(\sigma/\langle l\rangle)$ plateaus, similar results can be obtained using the clustering C_l, see Supplemental Material [13].

lattice node embeddings, respectively (see Supplemental Material [13] for 3D visualization). In the regular lattice, we introduce links with probability $p \sim 0.02$ between random unconnected pairs of nodes to obtain networks with high clustering and nonlocal connections as demonstrated in the examples of Fig. 4(a) (inset). Unlike our approach in one dimension, here we focus on the edge length distribution of the optimal graphs for different diffusive exponents.

As the random walk propagation speed decreases (β increases), both the average edge length $\langle l\rangle \equiv \sum_{i,j}^{N}(w_{ij}/W_{\text{tot}})l_{ij}$ and its coefficient of variation $\sigma/\langle l\rangle$ decrease in the optimal graphs. Ultimately, there is a transition from dense networks with long-range links to short-range sparse graphs with connections between geometrical nearest neighbors. If the nodes are regularly embedded and $\beta > \beta_c$, the optimum network forms a lattice of minimal edge length and zero length variance, see Fig. 4(a) (inset). The diffusive exponent at which the transition occurs depends on the embedding dimension as follows $\beta_c^{1D} > \beta_c^{2D} > \beta_c^{3D}$ [Fig. 4(b)].

We study random node embeddings by perturbing the nodes of regular lattices, see Fig. 4(a) (inset). Initially, the distribution of weights is uniform across all edges. However, after optimization shorter edges acquire larger weights than longer ones, reducing the average edge length. Particularly for $\beta \geq 0.5$, optimal search networks in randomized lattices achieve a lower average edge length than their regular lattice counterparts. This can affect the search efficiency since the average edge length establishes a lower bound on the graph search time. It can be shown using Jensen's inequality [34] for $\beta \geq 0.5$, that: $\langle l\rangle^{2\beta}[RW_{\text{tot}}/N(N-1)\mathcal{D}_\beta] \leq \langle T\rangle$.

To shed light on the crossover from dense to sparse optimal search graphs, we investigate when a shortcut addition can reduce the graph search time. Let G be a graph with N nodes approximately arranged on a D-dimensional hypercubic lattice with spacing $l_0 \simeq 1$, conductivity $c_0 = 1$, and weights $w_0 = 1$. The augmented graph $G + s_*$ has an additional shortcut s_*, connecting the lattice's opposite nodes with Euclidean distance $l_* \approx N^{(1/D)}$ and weight $w_* = (1/l_*)$. The addition of s_* always increases the total edge length and induces a travel time $(l_*^{2\beta}/\mathcal{D}_\beta)$. Conversely, s_* reduces the graph resistance $R_{+s_*} < R$ in line with Rayleigh's monotonicity law [19]. The shortcut is advantageous if

$$\frac{\langle T\rangle_{+s_*}}{\langle T\rangle} = \left(1 + \frac{2w_* l_*^{2\beta}}{\sum_{i,j}^{N} w_{ij} l_{ij}^{2\beta}}\right)\frac{R_{+s_*}}{R} < 1. \tag{4}$$

For a regular lattice with $N_e \propto N$ edges, inequality (4) becomes $\left(1 + \alpha N^{[(2\beta-1)/D]-1}\right)(R_{+s_*}/R) < 1$, where $\alpha > 0$ is a constant independent of N.

The improvement in graph resistance due to the addition of a shortcut between nodes (i, j), depends on how its weight compares to the effective weight of all paths between (i, j), denoted by $W_{ij} = R_{ij}^{-1}$. If the shortcut has a small weight (e.g., long length) or the graph is "loopy" with an inherently low average pairwise resistance, then $w_* R_{ij} \to 0$ for larger networks and the shortcut's improvement on the graph resistance gradually vanishes. For context, in one dimension, $R_{ij} \sim N$; in two dimensions, $R_{ij} \sim \log N$; and in three dimensions $R_{ij} \sim$ const [35,36].

Understanding how (R_{+s_*}/R) scales with the system size and the embedding dimension allows a prediction for the crossover exponent. However, an analytical estimation is challenging for noncirculant graphs (see Supplemental Material [13]). Instead, we can obtain a useful upper bound for the crossover β_c by observing that the graph resistance can reduce at most by $\left(R_{+s_*}/R\right) = \frac{1}{2}$, when s_* connects the antipodal nodes of a path graph G (edges in series) so that $G + s_*$ is converted into a cycle. From inequality (4), we obtain $\beta_c^D < [(D+1)/2]$, implying that as β increases, it becomes unfeasible to offset the diffusive delay. This agrees with the optimal search graphs depicted in Fig. 4(a) which prioritized minimizing the average edge length rather than maximizing connectivity.

Previously, diffusive search was classified based on its compactness [37–39]. If a random walk explores a graph of linear size $S = N^{1/d_f}$, where d_f is its fractal dimension, the exploration is compact if $2\beta > d_f$ and noncompact if $2\beta < d_f$. Our findings indicate that compactness alone is

not enough to capture the crossover of the optimal search architecture from long-range links to a short-range lattice. This transition depends on the type of diffusion, the system size, and the node embedding dimension as shown in Fig. 4(b). In one dimension, the crossover occurs asymptotically at $\beta = 1$ while the compactness changes at $\beta = 0.5$. In two dimensions, the compactness changes at $\beta = 1$ but the crossover is already observed for $\beta_c^{2D} < 1$ for the tested graphs up to $N \approx 10^4$. In three dimensions, the compactness changes for $\beta = 1.5$ but the crossover occurs for lower values, depending on the network size, e.g., for $N = 12^3$, $\beta_c^{3D} \approx 0.71$. Although our work focused on networks embedded in regular lattices and their perturbations, the crossover in the optimal search architecture should be examined for universality across different classes of networks, including fractal and scale-free graphs [39–41].

In this Letter, we investigated the topological and geometrical features for weighted and spatially heterogeneous networks that minimize the average mean first passage time between all node pairs. In physical network diffusion, the transit time through an edge depends on the edge's Euclidean length [11], and the propagation speed is determined by the type of anomalous random walk. As the epitome of this interplay, we find a Braess paradox analog, where for subdiffusion $\beta \geq 1$, extending the network with a shortcut between topologically distant nodes can worsen the overall search time if the link has a significant Euclidean length. However, a faster diffusive propagation, $\beta < \beta_c$, reduces the transit time, making topological shortcuts preferred.

Finding the optimal search architecture is crucial for transport efficiency in real-world networks and porous media [11,42]. To this end, we developed an optimization scheme under which each link adapts its conductivity to minimize the overall search time while conserving available resources. This process eliminates Braessian edges and enhances links that improve transport. The optimal search graph undergoes a crossover that depends on the diffusive exponent β and the embedding dimension. For $\beta < \beta_c^D$, we obtain dense graphs with long-range links, while for $\beta \geq \beta_c^D$ the optimal networks have short-range links between geometrical nearest neighbors. Our theory is broadly applicable since it is agnostic to the system-specific physics underlying diffusion. It requires only the scaling of the mean squared displacement within edges, node embedding, and graph topology. Therefore, it can offer insights across a range of systems that rely on diffusive transport in various length scales, including chemical reaction networks [37], intracellular networks [9], and microswimmers navigating mazes [43].

Acknowledgments—The authors would like to thank C. Doré, J. Khoury, A. Winn, and S. Wong for their insightful feedback. This research was supported by NSF Grant No. PHY-1554887, the University of Pennsylvania Materials Research Science and Engineering Center (MRSEC) through Grant No. DMR-1720530, and the Simons Foundation through Grant No. 568888.

[1] O. Bénichou, C. Loverdo, M. Moreau, and R. Voituriez, Intermittent search strategies, Rev. Mod. Phys. **83**, 81 (2011).
[2] A. L. Thorneywork, J. Gladrow, Y. Qing, M. Rico-Pasto, F. Ritort, H. Bayley, A. B. Kolomeisky, and U. F. Keyser, Direct detection of molecular intermediates from first-passage times, Sci. Adv. **6**, eaaz4642 (2020).
[3] J. Khoury and O. Parrikar, Search optimization, funnel topography, and dynamical criticality on the string landscape, J. Cosmol. Astropart. Phys. 12 (2019) 014.
[4] S. Redner, *A Guide to First-Passage Processes* (Cambridge University Press, Cambridge, England, 2001).
[5] A. Bassolas and V. Nicosia, First-passage times to quantify and compare structural correlations and heterogeneity in complex systems, Commun. Phys. **4**, 76 (2021).
[6] A. Ballal, W. B. Kion-Crosby, and A. V. Morozov, Network community detection and clustering with random walks, Phys. Rev. Res. **4**, 043117 (2022).
[7] L. Daqing, K. Kosmidis, A. Bunde, and S. Havlin, Dimension of spatially embedded networks, Nat. Phys. **7**, 481 (2011).
[8] D. J. Watts and S. H. Strogatz, Collective dynamics of 'small-world' networks, Nature (London) **393**, 440 (1998).
[9] A. Agrawal, Z. C. Scott, and E. F. Koslover, Morphology and transport in eukaryotic cells, Annu. Rev. Biophys. **51**, 247 (2022).
[10] V. Tejedor, O. Bénichou, and R. Voituriez, Global mean first-passage times of random walks on complex networks, Phys. Rev. E **80**, 065104(R) (2009).
[11] A. I. Brown, L. M. Westrate, and E. F. Koslover, Impact of global structure on diffusive exploration of organelle networks, Sci. Rep. **10**, 4984 (2020).
[12] D. Braess, A. Nagurney, and T. Wakolbinger, On a paradox of traffic planning, Transp. Sci. **39**, 446 (2005).
[13] See Supplemental Material at http://link.aps.org/supplemental/10.1103/PhysRevLett.133.067401, which includes Refs. [14–18] for the detailed derivation of Eq. 2 and a comprehensive study on the robustness of the optimization results. The supplemental material also includes an investigation into the impact of topological shortcuts on effective resistance. Additionally, we study the relationship between the edge length distribution of optimal graphs for different diffusive exponents.
[14] Francois Fouss, Alain Pirotte, Jean-Michel Renders, and Marco Saerens, Random-walk computation of similarities between nodes of a graph with application to collaborative recommendation, IEEE Trans. Knowl. Data Eng. **19**, 355 (2007).
[15] Piet van Mieghem, *Graph Spectra for Complex Networks* (Cambridge University Press, Cambridge, England, 2010).
[16] Jonathan R. Polimeni Leo J. Grady, *A Discrete Calculus Applied Analysis on Graphs for Computational Science* (Springer, London, 2010).

[17] Daniel J. Case, Yifan Liu, István Z. Kiss, Jean-Régis Angilella, and Adilson E. Motter, Braess's paradox and programmable behaviour in microfluidic networks, Nature (London) **574**, 647 (2019).
[18] Joel E. Cohen and Paul Horowitz, Paradoxical behaviour of mechanical and electrical networks, Nature (London) **352**, 699 (1991).
[19] P. G. Doyle and J. L. Snell, Random walks and electric networks, arXiv:math/0001057.
[20] Y. Lin and Z. Zhang, Random walks in weighted networks with a perfect trap: An application of Laplacian spectra, Phys. Rev. E **87**, 062140 (2013).
[21] R. Metzler and J. Klafter, The random walk's guide to anomalous diffusion: A fractional dynamics approach, Phys. Rep. **339**, 1 (2000).
[22] E. W. Montroll and H. Scher, Random walks on lattices. IV. Continuous-time walks and influence of absorbing boundaries, J. Stat. Phys. **9**, 101 (1973).
[23] D. S. Grebenkov and L. Tupikina, Heterogeneous continuous-time random walks, Phys. Rev. E **97**, 012148 (2018).
[24] A. Ghosh, S. Boyd, and A. Saberi, Minimizing effective resistance of a graph, SIAM Rev. **50**, 37 (2008).
[25] Z. Zhang, Y. Sheng, Z. Hu, and G. Chen, Optimal and suboptimal networks for efficient navigation measured by mean-first passage time of random walks, Chaos **22**, 043129 (2012).
[26] H. Youn, M. T. Gastner, and H. Jeong, Price of anarchy in transportation networks: Efficiency and optimality control, Phys. Rev. Lett. **101**, 128701 (2008).
[27] B. Schäfer, T. Pesch, D. Manik, J. Gollenstede, G. Lin, H.-P. Beck, D. Witthaut, and M. Timme, Understanding Braess' paradox in power grids, Nat. Commun. **13**, 5396 (2022).
[28] G. Gounaris, M. R. Garcia, and E. Katifori, Distribution efficiency and structure of complex networks, arXiv:2111.04657.
[29] S.-S. Chang and M. Roper, Microvascular networks with uniform flow, J. Theor. Biol. **462**, 48 (2019).
[30] J. Saramäki, M. Kivelä, J.-P. Onnela, K. Kaski, and J. Kertész, Generalizations of the clustering coefficient to weighted complex networks, Phys. Rev. E **75**, 027105 (2007).
[31] D. J. Watts and S. H. Strogatz, Collective dynamics of 'small-world' networks, Nature (London) **393**, 440 (1998).
[32] S. Kirkpatrick, C. D. Gelatt, and M. P. Vecchi, Optimization by simulated annealing, Science **220**, 671 (1983).
[33] D. J. Wales and J. P. K. Doye, Global optimization by basin-hopping and the lowest energy structures of Lennard-Jones clusters containing up to 110 atoms, J. Phys. Chem. A **101**, 5111 (1997).
[34] J. L. W. V. Jensen, Sur les fonctions convexes et les inégalités entre les valeurs moyennes, Acta Math. **30**, 175 (1906).
[35] W. Ellens, F. Spieksma, P. Van Mieghem, A. Jamakovic, and R. Kooij, Effective graph resistance, Linear Algebra Appl. **435**, 2491 (2011), special Issue in Honor of Dragos Cvetkovic.
[36] J. Cserti, Application of the lattice Green's function for calculating the resistance of an infinite network of resistors, Am. J. Phys. **68**, 896 (2000).
[37] O. Benichou, C. Chevalier, J. Klafter, B. Meyer, and R. Voituriez, Geometry-controlled kinetics, Nat. Chem. **2**, 472 (2010).
[38] P. G. de Gennes, Kinetics of diffusioncontrolled processes in dense polymer systems. I. Nonentangled regimes, J. Chem. Phys. **76**, 3316 (1982).
[39] S. Condamin, O. Bénichou, V. Tejedor, R. Voituriez, and J. Klafter, First-passage times in complex scale-invariant media, Nature (London) **450**, 77 (2007).
[40] L. K. Gallos, C. Song, S. Havlin, and H. A. Makse, Scaling theory of transport in complex biological networks, Proc. Natl. Acad. Sci. U.S.A. **104**, 7746 (2007).
[41] C. Song, S. Havlin, and H. A. Makse, Self-similarity of complex networks, Nature (London) **433**, 392 (2005).
[42] F. J. Meigel, T. Darwent, L. Bastin, L. Goehring, and K. Alim, Dispersive transport dynamics in porous media emerge from local correlations, Nat. Commun. **13**, 5885 (2022).
[43] T. V. Phan, R. Morris, M. E. Black, T. K. Do, K.-C. Lin, K. Nagy, J. C. Sturm, J. Bos, and R. H. Austin, Bacterial route finding and collective escape in mazes and fractals, Phys. Rev. X **10**, 031017 (2020).